Right ventricular volume load and function in congenital heart defects

Sverrir Stephensen, Sigurdur

2017

Document Version:
Publisher's PDF, also known as Version of record

Am J Physiol Heart Circ Physiol 306: H895–H903, 2014.
First published January 17, 2014; doi:10.1152/ajpheart.00483.2013.

The relationship between longitudinal, lateral, and septal contribution to stroke volume in patients with pulmonary regurgitation and healthy volunteers

Sigurdur Stephensen,[1,2] Katarina Steding-Ehrenborg,[1] Peter Munkhammar,[2] Einar Heiberg,[1,3] Hakan Arheden,[1] and Marcus Carlsson[1]

[1]*Department of Clinical Physiology and Nuclear Medicine, Lund University, Lund University Hospital, Lund, Sweden;* [2]*Department of Pediatric Cardiology, Lund University, Lund University Hospital, Lund, Sweden; and* [3]*Center for Mathematical Sciences, Lund University, Lund, Sweden*

Submitted 14 June 2013; accepted in final form 16 January 2014

Stephensen S, Steding-Ehrenborg K, Munkhammar P, Heiberg E, Arheden H, Carlsson M. The relationship between longitudinal, lateral, and septal contribution to stroke volume in patients with pulmonary regurgitation and healthy volunteers. *Am J Physiol Heart Circ Physiol* 306: H895–H903, 2014. First published January 17, 2014; doi:10.1152/ajpheart.00483.2013.—Septal systolic motion is towards the left ventricle (LV) in healthy hearts. Patients with pulmonary regurgitation (PR) and right ventricular (RV) volume overload have systolic septal motion toward the RV. This may affect the longitudinal contribution from atrioventricular plane displacement (AVPD) and septal and lateral contribution to stroke volume (SV). The study aimed to quantify these contributions to SV in patients with PR. Cardiac magnetic resonance imaging was used for assessment of cardiac volumes. Patients ($n = 30$; age 9–59 yr) with PR due to surgically corrected tetralogy of Fallot and 54 healthy controls (age 10–66 yr) were studied. Longitudinal contribution to RVSV was 47 ± 2% (means ± SE) in patients with PR and 79 ± 1% in controls ($P < 0.001$). Lateral contribution to RVSV and LVSV was 40 ± 1 and 62 ± 2% in patients and 31 ± 1 and 36 ± 1% in controls ($P < 0.001$ for both). Septal motion contributed to RVSV by 8 ± 1% in patients and by 7 ± 1% to LVSV in controls ($P < 0.001$). PR patients have decreased longitudinal contribution to RVSV and increased lateral pumping, resulting in larger outer volume changes and septal motion towards the RV. The changes in RV pumping physiology may be explained by RV remodeling resulting in lower systolic inflow of blood into the right atrium in relation to SV. This avoids the development of pendulum volume between the caval veins and right atrium, which would occur in PR patients if longitudinal contribution to SV was preserved. Decreased AVPD suggests that tricuspid annular excursion, a marker of RV function, is less valid in these patients.

septal motion; radial and longitudinal function; pulmonary regurgitation; RV volume load

LEFT VENTRICULAR (LV) PUMPING HAS been extensively studied but the function of the right ventricle (RV) remains less elucidated using cardiac MRI in determining regional contributions to stroke volume (SV) (20, 27). Understanding of RV function is of particular interest in patients with congenital heart disease. In a healthy adult heart, 60% of LVSV and 80% of RVSV are generated by longitudinal atrioventricular plane displacement (AVPD) (7, 8). The remaining part of the SV is contributed to by the radial function of the ventricles, through displacement of the lateral ventricular walls and the septum (29, 31). The contribution of lateral vs. septal displacement to left and RVSV is unknown. In healthy individuals the RV endocardial portion of the ventricular septum moves towards the left in systole, contributing to LVSV and to the right in diastole (16, 17). Patients with tetralogy of Fallot (TOF) often develop pulmonary regurgitation (PR) after surgical correction leading to a volume-loaded RV. This affects the septum, which moves towards the RV in systole (22) (Fig. 1) and through ventricular interdependence may even alter the longitudinal and lateral function of both ventricles. Cardiac magnetic resonance (CMR) has been validated and used to quantify the longitudinal and radial contribution to ventricular SV (7, 8). CMR can even quantify the lateral and septal aspects of the radial displacement in three dimensions, thereby quantifying their contribution to SV. The aim of this study was to quantify the contribution of longitudinal, lateral, and septal pumping to SV in pediatric and adult patients with RV volume overload, secondary to PR, and compare the results to healthy controls to explain the altered pumping mechanisms in a heart with volume-overloaded RV.

MATERIALS AND METHODS

Study population. The local ethics committee approved the study, and written informed consent was obtained from all patients before examination. Two groups of patients were studied: 15 children (8 females) and 15 adults (6 females) who had undergone corrective surgery for TOF ($n = 28$) or pulmonary stenosis ($n = 2$). The patients had varying degree of PR from 0 to 61%. RV systolic pressure was calculated from the maximum velocity of the tricuspid regurgitation (TR) jet on echocardiography (Table 1). The TR was mild in all but four patients, who had moderate TR. Two patients had moderate pulmonary valve stenosis, and three patients had moderate branch pulmonary artery stenosis. Effective RVSV was calculated by subtracting the PR volume, obtained from the flow analysis, from the RVSV obtained from the short-axis cine images (RVEDV-RVESV). Nine healthy children (3 females) and 45 healthy adult volunteers (25 females) with varying degrees of exercise level, to obtain a wide range of heart volumes, were used as controls.

CMR imaging. All subjects underwent CMR in the supine position, and images were acquired during end-expiratory breath hold covering the entire heart, including both ventricles and atria of the heart. A 1.5-Tesla CMR scanner with a five-element cardiac synergy coil was used for all studies (Philips Achieva, Best, The Netherlands). Steady-state free precession cine CMR images were acquired in the short-axis plane. Imaging parameters were typically: ECG triggering with acquired temporal resolution of 47 ms reconstructed to 30 time phases per cardiac cycle, repetition time 3 ms, echo time 1.4 ms, flip angle 60°, and slice thickness 5–8 mm with no slice gap. Breath-hold times were typically 15 s. The long axis images were acquired in the LV two chamber view, LV outflow tract view, and four-chamber view.

Flow analysis of the main pulmonary artery using phase velocity mapping was used to evaluate the regurgitant volume in the patients

Address for reprint requests and other correspondence: M. Carlsson, Dept. of Clinical Physiology and Nuclear Medicine, Lund Univ. Hospital, Lund Univ., SE-221 85 Lund, Sweden (e-mail: marcus.carlsson@med.lu.se).

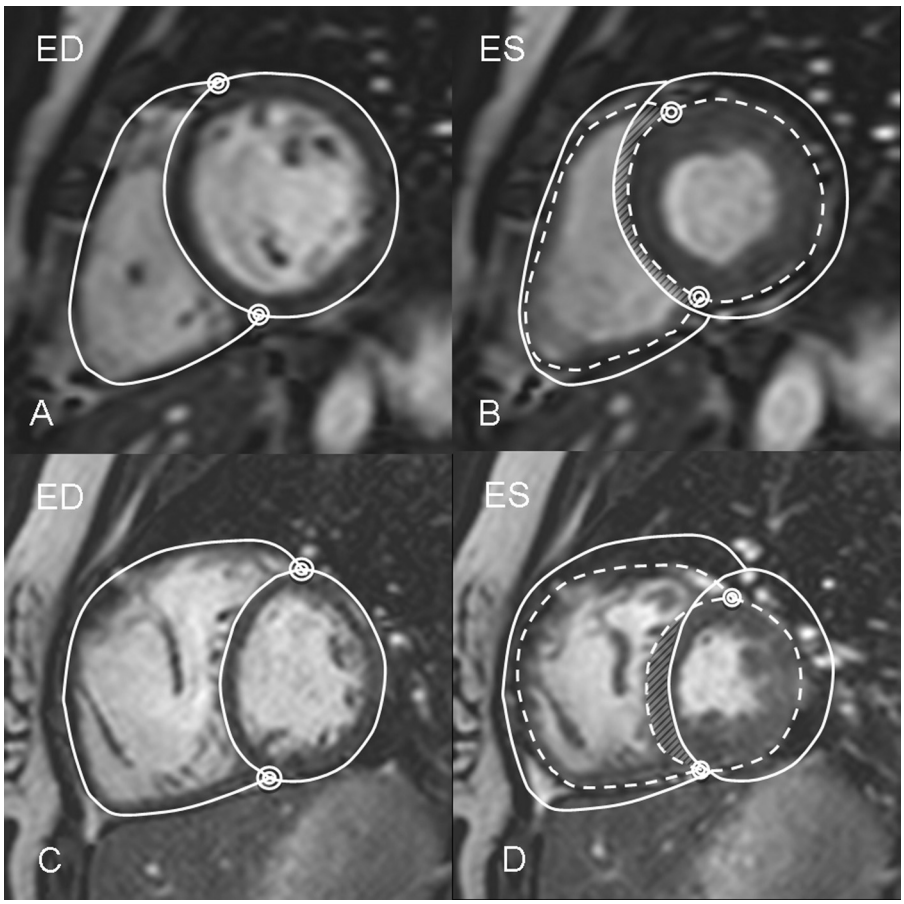

Fig. 1. Short axis view in end-diastole (ED) and end-systole (ES) in a healthy individual (*top row*) and a patient with severe pulmonary regurgitation (PR) secondary to tetralogy of Fallot (*bottom row*). The solid line represents the ED epicardial contour of the left (LV) and right ventricles (RV) and the broken line the ES epicardial contour. The 2 small double circles signify the anterior and inferior RV insertion points. The diastolic contour is copied to the systolic image to show how the septum moves toward the LV in systole in a healthy individual but to the RV in a patient with PR. The area demarcated by the ED and ES epicardial contours and the RV insertion points (diagonal lines) represents the volume contributed by the septal motion to the stroke volume (SV); a positive contribution to the LVSV in the healthy individual and a negative contribution to the LVSV in the patient with PR. This measurement was done in all short-axis slices from the base to the apex of the heart. In the same manner the contribution of the lateral wall displacement to LVSV and RVSV was calculated by using the 2 RV insertion points and the lateral LV and RV epicardial contours, respectively.

(21, 30). The flow images were acquired during free breathing using a fast field echo velocity encoded sequence with retrospective ECG triggering with repetition time 10 ms, echo time 5 ms, flip angle 15°, and slice thickness 8 mm, acquired in-plane resolution 2.4 × 2.4 mm reconstructed to 1.3 × 1.3 mm, with a 128 × 128 matrix, number of acquisitions 1, no parallel imaging, and a velocity encoding gradient (VENC) of 200 cm/s. The flow sequence was nonsegmented without echo sharing and had an acquired temporal resolution of 20 ms during the cardiac cycle with a scan time of 2 min and has been previously validated in vivo and in vitro (4).

Image analysis. All image analysis was performed using the segmentation software Segment, v1.9 R3025 (http://segment.heiberg.se) (14). LV and RVSV were obtained by delineating the endocardial borders of both ventricles in all slices in end-diastole (ED) and end-systole (ES).

Longitudinal contribution to SV for each ventricle was calculated as previously validated (7, 8). In short, the position of the AVP was determined by using eight location points in the three long axis images. The AVPD was calculated for each ventricle by subtracting the AVP position in ES from that in ED (Fig. 2) (7, 8). The mean of the two to three largest epicardial short-axis areas of the LV and the RV encompassed by the AVPD was multiplied by the AVPD to calculate the volume contributed to SV by the AVPD. The reason for using the epicardial area has been described by Carlsson et al. (8) by comparing the LV to a telescope, which shortens and lengthens along its long axis. On shortening, the telescope retains its outer diameter but the inner diameter decreases. The volume of the telescope as well as the ventricle decreases when the tube shortens, and this volume equals the SV. Given that the volume of the wall of the telescope, i.e., the myocardium is constant during the cardiac cycle, the only difference in volume between ED and ES must be that of what was inside the tube (ventricle), i.e., the blood.

Septal contribution to SV was quantified in the short axis images as shown in Fig. 1. The ventricular septum was defined by the LV

Table 1. *Subject characteristics*

	Healthy Children	Children with PR	Healthy Adults	Adults with PR
n	9	15	45	15
Mean age and range (yr)	14 ± 1 (10–17)	12 ± 1 (3–16)	32 ± 2 (21–66)	32 ± 8 (20–59)
Females, *n* (%)	3 (33)	8 (53)	19 (44)	6 (40)
BSA, m^2	1.5 ± 0.1	1.3 ± 0.1	1.9 ± 0.0	1.9 ± 0.1
Heart rate, beats/min	70 ± 3	75 ± 3	61 ± 1	68 ± 3*
RV pressure, mmHg		28 ± 2		34 ± 9
Indexed PR, ml/m^2		30 ± 4		25 ± 3
PR, %		41 ± 4		39 ± 3

Continuous variables are presented as means ± SE. PR, pulmonary regurgitation; BSA, body surface area; RV, right ventricle. *$P < 0.05$, when comparing patients with PR to healthy subjects.

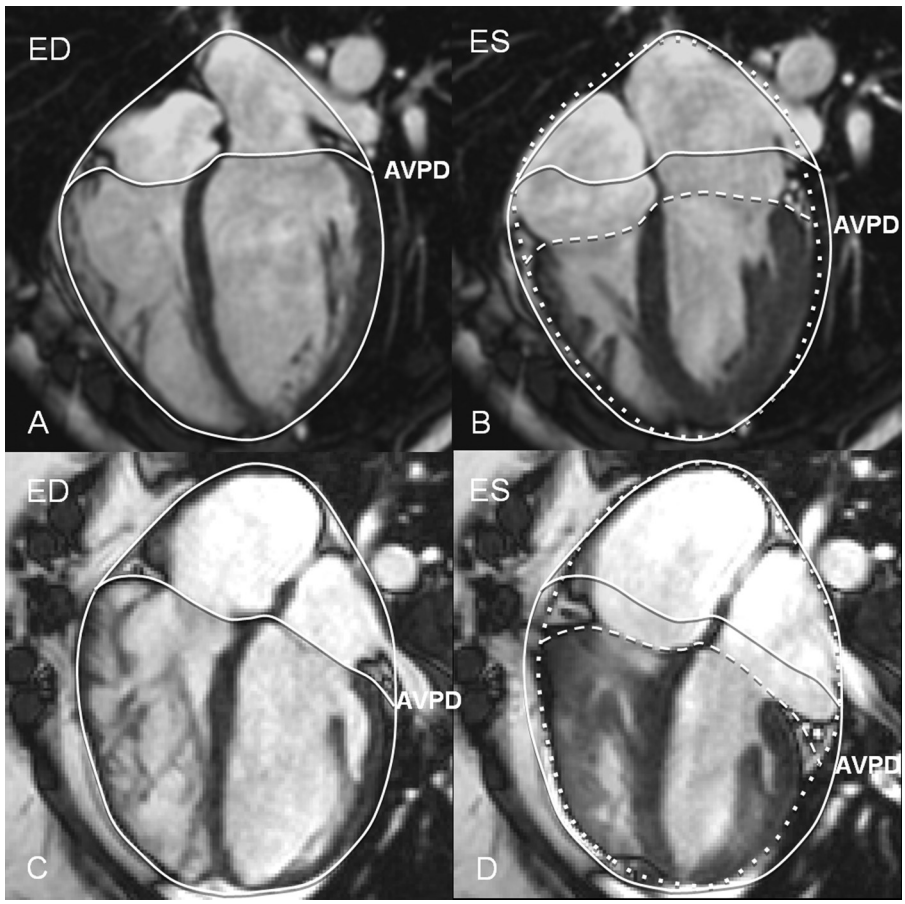

Fig. 2. Cardiac MR images in the 4-chamber view showing outer total heart volume variations in a healthy volunteer (*top row*) and a patient with severe PR secondary to tetralogy of Fallot (*bottom row*). The outer volume variations were larger in patients with PR compared with healthy volunteers. The solid and the dotted white lines represent the pericardial contours in ED and ES, respectively. Atrioventricular plane displacement (AVPD) is seen as a solid white line in ED and a dotted white line in ES. The AVPD of the LV is similar in the patient and the healthy subject, but AVPD of the RV is smaller in the patient than the healthy subjects.

epicardial border and the RV insertion points that mark the junction between the LV epicardium and RV epicardium; anteriorly at the junction of the anterior and anteroseptal segments and inferiorly at the junction of the inferior and inferoseptal segments of the LV. The epicardial contours of the LV in ED were copied to the corresponding images in ES in all slices from the base to the apex. This generated an area (diagonal lines in Fig. 1) that represents the volume contributed to SV by the septal movement. Septal motion towards the LV was denoted a positive contribution to the LVSV. Septal motion towards the RV was denoted a negative contribution to the LVSV or conversely a positive contribution to RVSV.

Lateral contribution to SV was calculated by copying the epicardial contours of the LV in ED to the ES images in all slices from the apex to the base as described above. The area demarcated by the lateral LV epicardial contours in ED and ES and the RV insertion points represents the volume contributed by the lateral displacement of the LV to LVSV. The same was done for the RV using the two RV insertion points and epicardial contours of the RV in ED and ES to calculate the volume contributed by the lateral displacement of the RV to RVSV (Fig. 1). At the base we only included the slices where both ventricles and the ventricular septum could be detected in both ED and ES to avoid including longitudinal displacement in the septal and lateral contribution to SV.

Wall thickness was measured in ED and ES and divided into septal and lateral walls of the LV. Wall thickening was calculated as (ES wall thickness − ED wall thickness)/ED wall thickness.

The center of volume (COV) of the heart was calculated using the delineation of total heart volume variation. This was performed by delineation of the pericardial border in short-axis images covering the whole heart (5, 6). All structures within the pericardium were included, ventricles, atrias, and the intrapericardial parts of the aorta and the pulmonary artery. The total heart volume was obtained in ED and ES by summation of all slices. The movement of the center of volume in three anatomical directions, septal-lateral, anterior-inferior, and apical-basal, between ED and ES was calculated to obtain center of volume variation (COVV) (6). A positive septal-lateral value denotes movement toward septum in systole, a positive anterior-inferior value denotes movement anteriorly in systole, and a positive apical-basal value denotes movement apically in systole.

Two observers delineated 24 subjects for interobserver variability.

Statistical analysis. All statistical analysis was performed using Graphpad Prism v 5.02. Continuous variables were presented as means ± SE. Pearson's correlation was used to examine the relationship between PR and longitudinal, lateral, and septal contribution to SV. A Mann-Whitney test was used to test if variables differed among the groups (longitudinal, lateral, and septal contribution to SV, wall thickening, and COVV). Results with a $P < 0.05$ were considered statistically significant.

RESULTS

Subject characteristics. Age, body surface area, heart rate, and RV pressure measured echocardiographically through TR and regurgitation fraction of the patients with PR are presented in Table 1. Interobserver variability was 2 ± 2 ml or 1 ± 1% for LVSV, 7 ± 2 ml or 5 ± 1% for RVSV, 10 ± 1% for LVAVPD, and 2 ± 2% for RVAVPD. LV volumes and function are presented in Table 2. RV volumes and function are presented in Table 3.

Table 2. *Left ventricular size and function*

	Healthy Children	Children with PR	Healthy Adults	Adults with PR
LVEDVi, ml/m^2	106 ± 5	91 ± 4*	106 ± 3	94 ± 4*
LVESVi, ml/m^2	47 ± 3	41 ± 2	44 ± 1	45 ± 2
LVSVi, ml/m^2	59 ± 3	50 ± 2*	62 ± 2	48 ± 2‡
LVEF, %	56 ± 1	55 ± 2	59 ± 1	51 ± 1†
Cardiac index, l·min^{-1}· m^{-2}	4.1 ± 0.2	3.7 ± 0.2	3.7 ± 0.1	3.3 ± 0.2*
Indexed longitudinal contribution to LVSV (LVAVPDi), ml/m^2	30 ± 2	26 ± 2	38 ± 1	26 ± 2‡
Longitudinal contribution to LVSV, %	50 ± 2	54 ± 4	61 ± 1	55 ± 2*
Indexed radial contribution to total SV (THVVi), ml/m^2	40 ± 2	73 ± 4‡	33 ± 2	68 ± 5‡
Radial contribution to total SV, %	36 ± 3	58 ± 2‡	26 ± 1	59 ± 2‡
Indexed lateral contribution to LVSV, ml/m^2	23 ± 1	34 ± 2†	22 ± 1	28 ± 2*
Lateral contribution to LVSV, %	40 ± 3	67 ± 3‡	36 ± 1	58 ± 3‡
Indexed septal contribution to SV, ml/m^2	3 ± 1	−6 ± 1‡	5 ± 0	−6 ± 1‡
Septal contribution to SV, %	5 ± 1	−8 ± 1‡	8 ± 0	−8 ± 1‡

Continuous variables are presented as means ± SE. LVEDVi, left ventricular end diastolic volume indexed to BSA; LVESVi, left ventricular end systolic volume indexed to BSA; LVSVi, left ventricular stroke volume indexed to BSA; LVEF, left ventricular ejection fraction; LVAVPD, left ventricular atrioventricular plane displacement; THVV, total heart volume variation. Septal contribution to LVSV is denoted a positive number and septal contribution to RVSV is denoted a negative number. *$P < 0.05$, †$P < 0.01$, ‡$P < 0.001$, when comparing patients with PR to healthy subjects.

The effective RVSV was significantly lower both in children ($P < 0.01$) and adults ($P < 0.001$) with PR compared with controls (Table 3).

Longitudinal pumping–contribution of AVPD to SV. Indexed atrioventricular plane displacement (AVPDi) was lower in adult patients with PR compared with healthy adults in both LV and RV ($P < 0.001$ for both). AVPDi in children with PR was smaller in the RV ($P < 0.01$) but not the LV ($P = 0.15$) compared with healthy children (Tables 2 and 3).

The contribution of AVPD to LVSV was slightly lower in adult patients with PR compared with healthy adults ($P < 0.05$), but there was no difference between pediatric patients and healthy children ($P = 0.36$; Tables 2 and 3 and Fig. 3*A*). Longitudinal contribution to LVSV in healthy children was lower than in healthy adults ($P < 0.01$).

In contrast to the LV, the contribution of AVPD to RVSV was considerably lower in patients with PR compared with healthy subjects ($P < 0.001$; Fig. 3*B*).

The contribution of longitudinal function to SV was not related to RV size (RVEDVi) in patients ($P = 0.62$ for LVAVPD and $P = 0.90$ for RVAVPD) or healthy subjects ($P = 0.25$ for LVAVPD and $P = 0.21$ for RVAVPD).

Lateral pumping. Lateral contribution to LVSV was significantly larger in patients with PR (67 ± 3% in children and 58 ± 3% in adults) compared with healthy subjects (40 ± 3% in children and 36 ± 1% in adults; $P < 0.001$ for both; Table 2 and Fig. 4*A*).

Lateral contribution to RVSV was significantly larger in adult patients with PR than healthy subjects ($P < 0.001$), but there was no significant difference between children with PR and healthy children ($P = 0.07$; Table 3 and Fig. 4*B*).

The contribution of LV lateral function correlated with RV size (RVEDVi) in patients ($r = 0.38$; $R^2 = 0.14$; $P < 0.05$) but not in healthy subjects ($P = 0.06$). There was no correlation between RV lateral function and RV size (RVEDVi) in patients or healthy subjects ($P = 0.86$ and $P = 0.20$, respectively).

Contribution of septal motion to SV. Ventricular septal displacement contributed to LVSV in all healthy controls (Table 2). In all but one patient with PR, the ventricular septum contributed to RVSV. Septal motion contributed by 7 ± 1% to LVSV in healthy controls of all ages. In patients with PR, however, septal motion contributed by 8 ± 1% to the RVSV ($P < 0.001$ compared with healthy controls; Fig. 5).

The contribution of the septal movement to SV was not related to RV size in patients ($P = 0.80$ for RVEDVi) or healthy controls ($P = 0.34$ for RVEDVi). In patients with PR there was no correlation between septal contribution to RVSV and other components of RV size or function such as RVESVi ($P = 0.98$) or RV ejection fraction (EF; $P = 0.62$).

Table 3. *Right ventricular size and function*

	Healthy Children	Children with PR	Healthy Adults	Adults with PR
RVEDVi, ml/m^2	112 ± 7	169 ± 10†	117 ± 3	157 ± 10‡
RVESVi, ml/m^2	55 ± 4	94 ± 8†	53 ± 2	91 ± 8‡
RVSVi, ml/m^2	57 ± 3	75 ± 4†	64 ± 2	65 ± 5
RVEF, %	51 ± 1	45 ± 2	55 ± 1	42 ± 3‡
Indexed longitudinal contribution to RVSV (RVAVPDi), ml/m^2	45 ± 3	33 ± 2†	51 ± 2	32 ± 3‡
Longitudinal contribution to RVSV, %	79 ± 3	45 ± 2‡	79 ± 1	49 ± 3‡
Indexed lateral contribution to RVSV, ml/m^2	19 ± 2	30 ± 2†	19 ± 1	26 ± 2†
Lateral contribution to RVSV, %	33 ± 3	40 ± 2	30 ± 1	40 ± 2‡
Indexed effective RVSV, ml/m^2	57 ± 3	45 ± 3†	64 ± 2	40 ± 3‡
RVEF corr, %		28 ± 2		27 ± 2

Continuous variables are presented as means ± SE. RVEDVi, right ventricular end diastolic volume indexed to BSA; RVESVi, right ventricular end systolic volume indexed to BSA; RVSVi, right ventricular stroke volume indexed to BSA; RVEF, right ventricular ejection fraction; RVAVPD, right ventricular atrioventricular plane displacement; Indexed effective RVSV = (RVSV-PR)/BSA; RVEF corr, RVEF corrected for pulmonary regurgitation. †$P < 0.01$, ‡$P < 0.001$, when comparing patients with PR to healthy subjects.

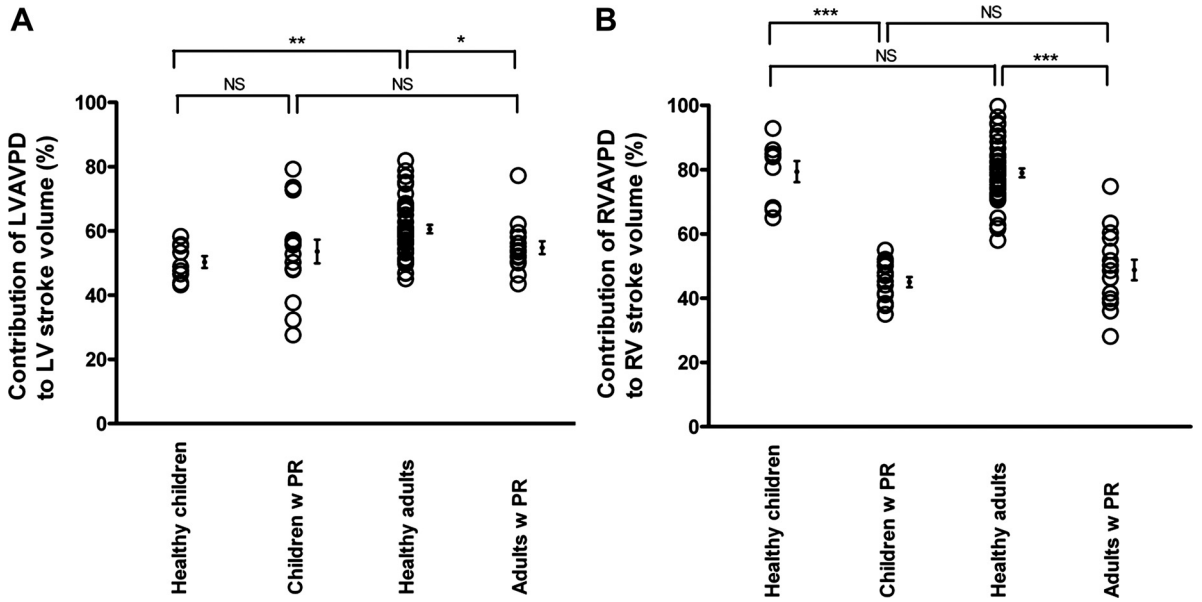

Fig. 3. Contribution of the AVPD to LVSV (*A*) and RVSV (*B*) in healthy adults and children and adults and children with PR. $*P < 0.05$, $**P < 0.01$, $***P < 0.001$.

Sum of components of SV. When adding the longitudinal, lateral, and septal contributions to SV the sums were 103 ± 1% for LVSV and 103 ± 1% for RVSV in healthy subjects and 105 ± 2% for LVSV and 95 ± 2% for RVSV in patients.

Pulmonary regurgitation. The volume of the PR correlated with: the volume contributed to SV by RVAVPD ($r = 0.52$; $R^2 = 0.27$; $P < 0.01$; Fig. 6*A*), the volume contributed by lateral displacement to LVSV ($r = 0.58$; $R^2 = 0.34$; $P < 0.001$; Fig. 6*B*) and RVSV ($r = 0.69$; $R^2 = 0.47$; $P < 0.001$; Fig. 6*C*), and the volume contributed to SV by septal displacement ($r = 0.42$; $R^2 = 0.18$; $P < 0.05$; Fig. 6*D*).

Wall thickening and center of volume variation. Wall thickening between ED and ES was lower in patients with PR than healthy subjects ($P < 0.01$). There was no difference between septal (53 ± 4%) and lateral (52 ± 3%; $P = 0.8$) wall thickening in patients. A small but significant difference was found between septal (67 ± 2%) and lateral (62 ± 2%; $P < 0.05$) wall thickening in healthy subjects.

COVV in patients did not differ from healthy subjects in the septal direction (1.8 ± 0.2 vs. 1.5 ± 0.1 mm; $P = 0.31$) or in the anterior direction (0.1 ± 0.3 vs. 0.6 ± 0.1 mm; $P = 0.53$), but there was a larger movement in the basal direction in patients compared with healthy subjects (4.6 ± 0.3 vs. 2.6 ± 0.2 mm; $P < 0.001$).

DISCUSSION

This study has shown that the RVSV in adult and pediatric patients with PR is generated to a larger extent by radial pumping compared with healthy subjects. This manifests in-

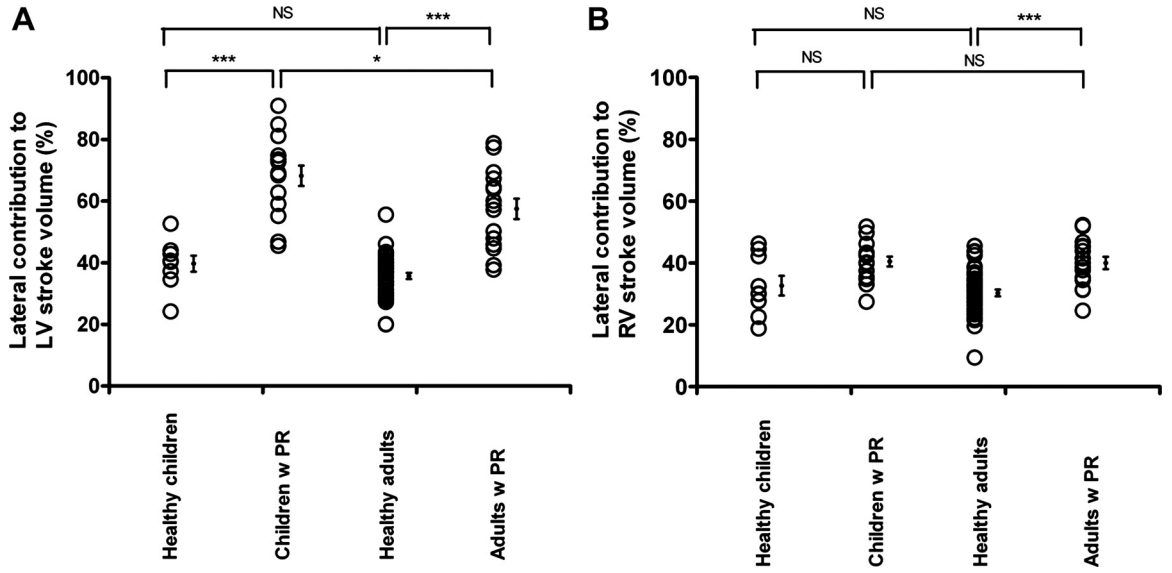

Fig. 4. Lateral contribution to LVSV (*A*) and RVSV (*B*) in healthy adults and children and adults and children with PR. $*P < 0.05$, $***P < 0.001$.

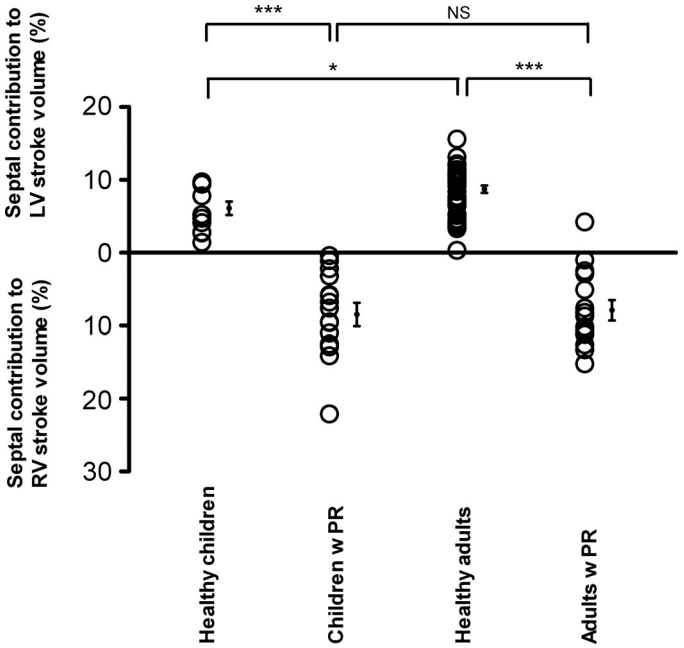

Fig. 5. Contribution of the ventricular septal movement to LVSV in healthy adults and children and to right RV systolic SV in adults and children with PR. $*P < 0.05$, $**P < 0.01$, $***P < 0.001$.

ternally as septal motion towards the RV and externally as outer volume changes because of inward motion of the lateral walls of the RV and LV. The AVPD, or longitudinal pumping, in patients with PR contributes to a lesser degree to RVSV compared with healthy subjects. The volume overload caused by PR thus causes changes in pumping physiology that may be explained by RV remodeling. The lower contribution of AVPD to RVSV implies that the echocardiographic assessment of tricuspid annular plane systolic excursion, as the marker of RV function, is less valid in patients with volume overload due to PR. The contribution of AVPD to LV pumping, however, is unchanged in patients with PR. Moreover, this study has quantified the contribution of septal motion to SV in healthy subjects and patients with PR. Interestingly, the study also found differences in the contribution of longitudinal and lateral displacement to LVSV between healthy adults and healthy children.

Physiological mechanisms. Figure 7 shows schematic drawings of RV pumping in a normal subject and in a patient with PR to explain the differences in radial and longitudinal pumping. In a healthy subject, where RVSV is equal to LVSV, the longitudinal contribution to RVSV is 80%. In systole, the longitudinal displacement of the AV plane towards the apex causes subsequent atrial filling of equal volume, i.e., 80% of the RVSV (28). In a patient with moderate PR, where systolic RVSV is significantly larger than LVSV (Tables 2 and 3), preserved longitudinal contribution, of 80% of RVSV, would result in a systolic inflow to the right atrium larger than the effective SV (RVSV-PR). This theoretical example would in turn result in a volume expanded right atrium and a pendulum volume of blood between the right atrium and the caval veins. The decreased longitudinal contribution to RVSV prohibits these effects.

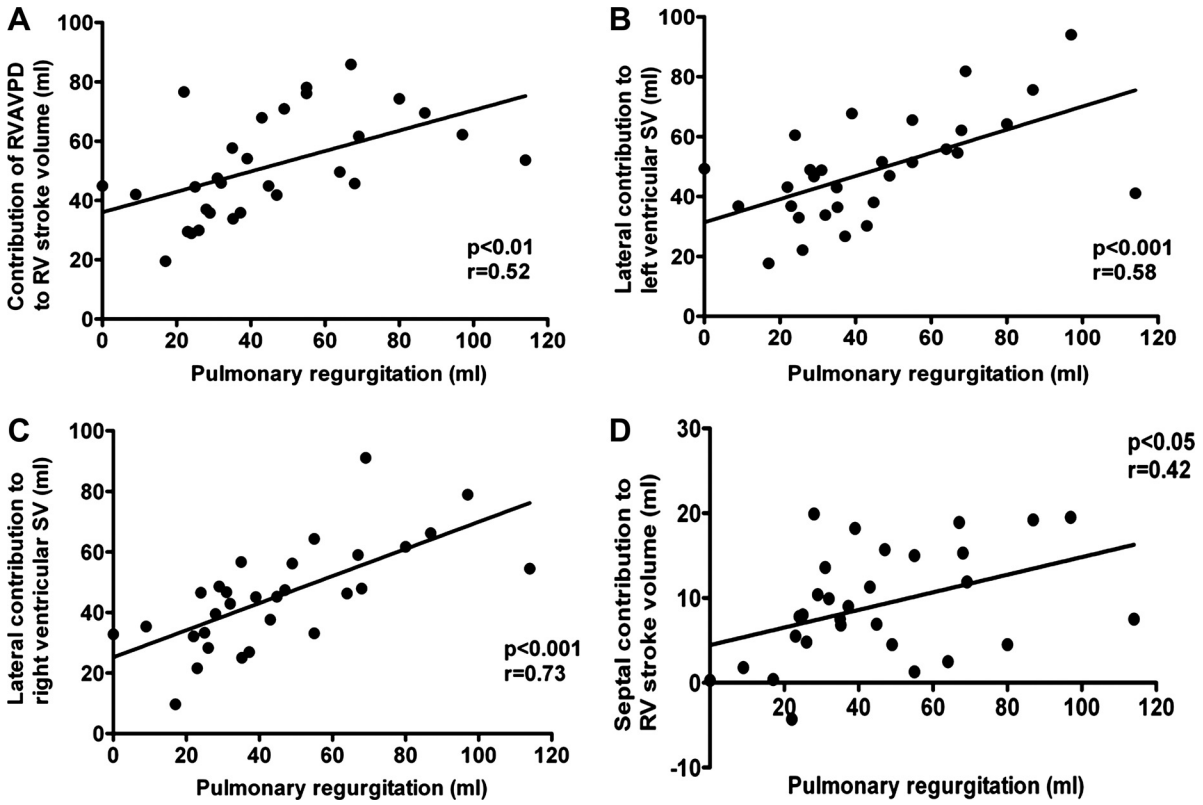

Fig. 6. Correlation between PR and contribution of RVAVPD to SV (*A*), contribution of lateral displacement to LVSV (*B*), contribution of lateral displacement to RVSV (*C*), and contribution of septal movement to RVSV.

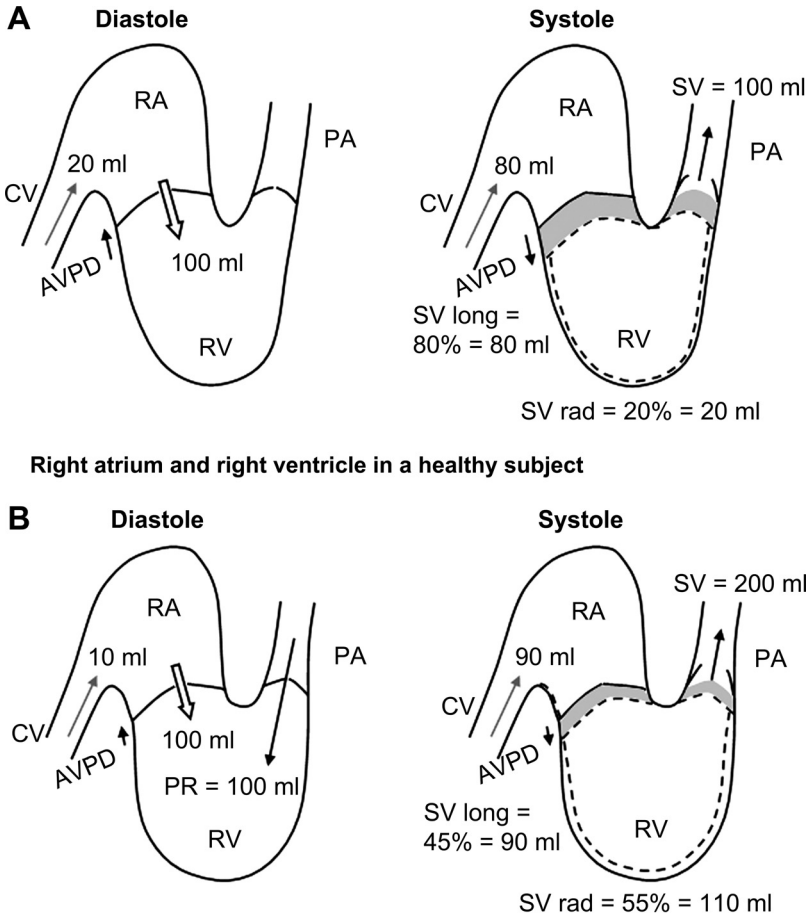

Fig. 7. Schematic long-axis illustration of the inflow and the outflow of the RV, explaining the relationship between longitudinal and radial function in a normal RV and a volume overloaded RV secondary to PR. The outer contour of the heart is shown as a solid line in diastole and as a dotted line in systole. The AVPD is towards the base of the heart in diastole, the blood flows from the right atrium (RA) to the RV (open arrow) and simultaneously blood enters the RA from the caval veins (grey arrow). In systole the AVPD is towards the apex, the right ventricular SV is shown at the pulmonary artery (PA) and simultaneously blood enters the RA from the caval veins (CV). The numbers shown in percent represent the longitudinal (SV long) and radial (SV rad) contribution to SV. *A*: RA and RV in a normal subject. Net inflow from the caval veins to the RA is 100 ml; 20 ml in diastole and 80 ml in systole. In diastole 100 ml of blood are drawn in from the RA to the RV. SV is 100 ml where 80% or 80 ml is generated by the AVPD (SV long) and 20% or 20 ml is generated by the radial displacement (SV rad). *B*: RA and RV of a patient with PR of 100 ml, dilated RV, and longitudinal and radial function as we have observed in the study. In diastole 100 ml of blood are drawn in from the RA to the RV but at the same time there is a PR of 100 ml from the PA to the RV. The SV is thus twice as big as in the normal subject or 200 ml. The radial contribution (SV rad) is larger, contributing to 55% of the SV or 110 ml. The AVPD (SV long) is decreased, only contributing to 45% or 90 ml of the SV. This prompts the same amount of 90 ml to be drawn in from the caval veins to the RA in systole and 10 ml in diastole.

Previous studies have described the physiological relationship between radial and longitudinal function in the normal heart (1, 2, 5, 6, 7, 31) as well as in the dysfunctional LV (8, 25). Coghlan and Hoffman (11) described the helical structure of the myofibers with a 56–60° angle between them as the optimal structure in the LV to endure the internal pressure of the blood and at the same time shorten adequately to eject the blood. This architectural pattern is altered in the diseased heart, which takes on a more dilated, spherical form and loses pumping efficiency. It is uncertain if those results can be transferred directly to the RV, which has different structure, different embryonic origin (32), and different adaptation to stress (15). However, a similar shift in RV contraction pattern has been described by Petterson et al. (24) in patients with a systemic RV. They studied myocardial strain by CMR tagging in Senning-operated patients with transposition of the great arteries. In these patients, who have RV pressure overload, the shortening pattern changes toward that of a LV with predominant circumferential contraction and less longitudinal shortening. A possible explanation for the changes we have observed in our study is that the volume overload, caused by the regurgitation volume from the pulmonary artery, leads to stretching of myofibers with subsequent distorted meshwork, more spherical architecture, and overexpansion of the RV similar to a pressure-loaded LV. These structural changes might alter the contraction pattern to a greater radial contribution, limit the movement of the AV plane in diastole, and conversely decrease the systolic inflow of blood (Fig. 7). These adaptational changes would thereby cause a better matching of the inflow to the heart with the net outflow from the RV, i.e., the RVSV minus the regurgitant volume from the pulmonary artery.

Increased RVED volume index in patients after repair for TOF is associated with elevated LVED pressure (26). The volume-loaded RV in these patients leads to distortion of the RV endocardial portion of the ventricular septum, which moves to the left in diastole, limiting the filling of the LV during atrial contraction (18). In systole the ventricular septum moves paradoxically towards the RV (22), thereby contributing to the RVSV but subtracting the same volume from the LVSV. This means that to preserve the LVSV either the AV plane or the LV lateral wall must compensate for the lack of septal contribution to LVSV. Even though there was no correlation between RV size and septal contribution to RVSV, we found a correlation between RV size and the contribution of the LV lateral wall to LVSV in the patient group.

Adult patients with PR had lower LVAVPD than healthy subjects, but the percent contribution of AVPD to the LVSV was the same in both groups, explained by the lower effective SV in patients compared with healthy subjects. The lower

LVSV is probably explained by a lower RVSV compensated with a higher heart rate compared with controls. The loss of septal contribution to LVSV in adult patients with PR was not compensated by increased longitudinal contribution to LVSV but rather by the increased displacement of the LV lateral wall as explained above. Although the adult patients had LVEF within the normal range (50–65%), it was significantly lower than in the group of healthy adults. The cardiac index in the adult patient group was also significantly lower than in the group of healthy adults ($P < 0.05$; Table 2). Impaired regional LV function in Fallot patients as demonstrated by the decreased radial thickening in both the septum and lateral wall in the presence of normal LVEF is in line with previous findings by Ordovas et al. (23).This is the first study to quantify the contribution of the ventricular septal movement to SV. In healthy subjects the ventricular septum contributes to 7% of the LVSV, whereas in patients with PR and paradoxical septal motion, the septum contributes to 8% of the RVSV. It is likely that a large number of TOF patients have some degree of paradoxical septal motion that is unrelated to RV size and PR volume but rather related to factors such as fibrosis of the RV insertion points leading to increased mechanical stress in these places as suggested by Muzzarelli et al. (22). A recent study by Chalard et al. (9) found decreased septal motion towards the RV after pulmonary valve replacement.

A possible mechanism behind the septal movement could be translational bulk motion of the LV from left to right. This would be more likely in patients with a large RV and also be related to adhesions of the RV pericardium to the sternum after cardiac surgery. In that scenario septal movement would be passive instead of contributing to RVSV by active contraction. To determine if this was the case we measured systolic wall thickening but found no differences between the septum and lateral wall in patients with PR. Furthermore, measurement of the center of volume variation between diastole and systole showed that COVV in the septal and anterior direction was similar in patients compared with healthy subjects. The lateral inward movement of the RV anterior, lateral, and diaphragmal walls was preserved in children and even increased in adult patients with PR compared with healthy subjects, making pericardial adhesions unlikely.

The sum of the longitudinal, lateral, and septal components of SV for both LV and RV should be 100% serving as an internal validation. In our results the sums of these three components were 103% in controls and 105% for LVSV and 95% for RVSV in patients with PR, which furthermore supports the notion that septal movement is an active process contributing to RVSV in patients with PR and not a passive effect of a bulk motion.

Measurements of regional strain with velocity-encoded MRI and echocardiography speckle tracking are used to assess myocardial function. LV global longitudinal strain in healthy subjects measured with MR was 18% in a recent article by Heiberg et al. (13), and in a study on patients with TOF by Lu et al. (19) longitudinal strain in the LV was 15% and in the RV free wall 18%. Of note, this should not be thought of as the percent longitudinal contribution to SV. Rather, the complex arrangement of myocardial fibers in different directions will combine in a net result of a longitudinal shortening that causes 60% of the SV in a healthy LV and 80% in a healthy RV. This can be compared with how a 15% shortening of myofiber will cause an EF of 60% (10). Therefore, regional measurements of, e.g., longitudinal strain cannot be used directly to explain the longitudinal contribution to SV, which is the net global result of said regional myocardial shortening.

Previous studies of ventricular interaction, mediated through the ventricular septum (18, 12) and the abnormal excursion of the septum in patients operated for TOF (22), did not quantify the volume generated by the septal displacement. This study has described a method that can be used to study ventricular interaction in different patient categories using conventional short axis images. The septal movement is a part of the radial shortening and, as such, has an important role in the contraction of the volume loaded RV.

A novel and unexpected finding in this study is the difference in pumping physiology between healthy children and healthy adults. The children had smaller longitudinal and septal contribution to LVSV than adults, but the lateral contribution to LVSV did not differ. A possible mechanism may be the lower LV mass found in children compared with adults (3), but further studies are needed to explain this finding.

Further studies. We included patients with RV volume overload due to a PR secondary to operated TOF or pulmonary stenosis. Further studies will show if the RV adapts to volume overload by decreased longitudinal function and increased septal and lateral contribution to RVSV in other conditions with a dilated RV, for example, patients with significant atrial septal defects. If present in those patients, one could exclude the PR as a contributing factor to the decreased AVPD as well as the influence of prior surgery and cardiopulmonary bypass on the heart function.

Limitations. When calculating longitudinal and radial contribution to SV we have measured these variables independently of each other. We have thus not taken into account that in the most basal part there is a simultaneous longitudinal and radial displacement of the ventricle. The radial contribution of the SV in the most basal part is not included in our analysis, and therefore, the radial contribution may be slightly underestimated. However, since the sum of the longitudinal, lateral, and septal components of SV was close to 100%, this limitation is probably of negligible magnitude.

When assessing the regional function of the septum and the lateral wall, we used wall thickening between diastole and systole. Future studies could include more advanced wall function methods such as tagging or tissue velocity mapping.

Conclusion. Patients with PR and RV volume overload have increased radial and decreased longitudinal contribution to RVSV compared with healthy subjects. The PR and the volume overload likely lead to remodeling of the RV with altered pumping mechanism. The longitudinal contribution to RVSV in patients with PR is lower, which limits the systolic inflow of blood to the heart and subsequently avoids the development of a pendulum volume between the caval veins and the right atrium. Instead, the increased lateral displacement of the free wall as well as septal motion toward the RV contributes to a larger extent to the RVSV. The LVAVPD in patients is unchanged even though the paradoxical septal movement subtracts volume from the LVSV. Increased LV lateral wall motion compensates for the "loss" of LVSV due to septal motion in patients with PR. This study also showed an unexpected lower longitudinal and septal contribution to SV in

healthy children compared with adults that warrants further investigation.

ACKNOWLEDGMENTS

We thank the technicians Christel Carlander and Ann-Helen Arvidsson for assistance in data collection.

GRANTS

This work was funded by the Swedish Research Council (2008-2461 and 2008-2949), Swedish Heart-Lung Foundation, Medical Faculty of Lund University, and Region of Scania.

DISCLOSURES

No conflicts of interest, financial or otherwise, are declared by the author(s).

AUTHOR CONTRIBUTIONS

Author contributions: S.S.S., E.H., H.A., and M.C. conception and design of research; S.S.S., K.S.-E., P.M., E.H., and M.C. performed experiments; S.S.S., K.S.-E., P.M., E.H., and M.C. analyzed data; S.S.S., K.S.-E., E.H., and M.C. interpreted results of experiments; S.S.S. prepared figures; S.S.S. drafted manuscript; S.S.S., H.A., and M.C. edited and revised manuscript; S.S.S., K.S.-E., P.M., E.H., H.A., and M.C. approved final version of manuscript.

REFERENCES

1. **Bowman AW, Kovács SJ.** Assessment and consequences of the constant-volume attribute of the four-chambered heart. *Am J Physiol Heart Circ Physiol* 285: H2027–H2033, 2003.
2. **Bowman AW, Kovács SJ.** Left atrial conduit volume is generated by deviation from the constant-volume state of the left heart: a combined MRI-echocardiographic study. *Am J Physiol Heart Circ Physiol* 286: H2416–H2424, 2004.
3. **Cain PA, Ahl R, Hedstrom E, Ugander M, Allansdotter-Johnsson A, Friberg P, Marild S, Arheden H.** Physiological determinants of the variation in left ventricular mass from early adolescence to late adulthood in healthy subjects. *Clin Physiol Funct Imaging* 27: 255–262, 2007.
4. **Carlsson M, Andersson R, Bloch K, Steding-Ehrenborg K, Mosén H, Stahlberg F, Ekmehag B, Arheden H.** Cardiac output and cardiac index measured with cardiovascular magnetic resonance in healthy subjects, elite athletes and patients with congestive heart failure. *J Cardiovasc Magn Reson* 14: 51, 2012.
5. **Carlsson M, Cain P, Holmqvist C, Stahlberg F, Lundback S, Arheden H.** Total heart volume variation throughout the cardiac cycle in humans. *Am J Physiol Heart Circ Physiol* 287: H243–H250, 2004.
6. **Carlsson M, Rosengren A, Ugander M, Ekelund U, Cain PA, Arheden H.** Center of volume and total heart volume variation in healthy subjects and patients before and after coronary bypass surgery. *Clin Physiol Funct Imaging* 25: 226–233, 2005.
7. **Carlsson M, Ugander M, Heiberg E, Arheden H.** The quantitative relationship between longitudinal and radial function in left, right, and total heart pumping in humans. *Am J Physiol Heart Circ Physiol* 293: H636–H644, 2007.
8. **Carlsson M, Ugander M, Mosén H, Buhre T, Arheden H.** Atrioventricular plane displacement is the major contributor to left ventricular pumping in healthy adults, athletes, and patients with dilated cardiomyopathy. *Am J Physiol Heart Circ Physiol* 292: H1452–H1459, 2007.
9. **Chalard A, Sanchez I, Gouton M, Henaine R, Salami FA, Ninet J, Douek PC, Di Filippo S, Boussel L.** Effect of pulmonary valve replacement on left ventricular function in patients with tetralogy of fallot. *Am J Cardiol* 110: 1828–1835, 2012.
10. **Cheng A, Nguyen TC, Malinowski M, Daughters GT, Miller DC, Ingels NB.** Heterogeneity of left ventricular wall thickening mechanisms. *Circulation* 118: 713–721, 2008.
11. **Coghlan C, Hoffman J.** Leonardo da Vinci's flights of the mind must continue: cardiac architecture and the fundamental relation of form and function revisited. *Eur J Cardiothorac Surg* 29: S4–S17, 2006.
12. **Damiano RJ Jr, La Follette P Jr, Cox JL, Lowe JE, Santamore WP.** Significant left ventricular contribution to right ventricular systolic function. *Am J Physiol Heart Circ Physiol* 261: H1514–H1524, 1991.
13. **Heiberg E, Pahlm-Webb U, Agarwal S, Bergvall E, Fransson H, Steding-Ehrenborg K, Carlsson M, Arheden H.** Longitudinal strain from velocity encoded cardiovascular magnetic resonance: a validation study. *J Cardiovasc Magn Reson* 15: 15, 2013.
14. **Heiberg E, Sjögren J, Ugander M, Carlsson M, Engblom H, Arheden H.** Design and validation of segment–freely available software for cardiovascular image analysis. *BMC Med Imaging* 10: 1, 2010.
15. **Kaufman BD, Desai M, Reddy S, Osorio JC, Chen JM, Mosca RS, Ferrante AW, Mital S.** Genomic profiling of left and right ventricular hypertrophy in congenital heart disease. *J Card Fail* 14: 760–767, 2008.
16. **Kaul S.** The interventricular septum in health and disease. *Am Heart J* 112: 568–581, 1986.
17. **Lima JA, Guzman PA, Yin FC, Brawley RK, Humphrey L, Traill TA, Lima SD, Marino P, Weisfeldt ML, Weiss JL.** Septal geometry in the unloaded living human heart. *Circulation* 74: 463–468, 1986.
18. **Louie EK, Rich S, Levitsky S, Brundage BH.** Doppler echocardiographic demonstration of the differential effects of right ventricular pressure and volume overload on left ventricular geometry and filling. *J Am Coll Cardiol* 19: 84–90, 1992.
19. **Lu JC, Ghadimi Mahani M, Agarwal PP, Cotts TB, Dorfman AL.** Usefulness of right ventricular free wall strain to predict quality of life in "repaired" tetralogy of Fallot. *Am J Cardiol* 111: 1644–1649, 2013.
20. **Mertens LL, Friedberg MK.** Imaging the right ventricle–current state of the art. *Nat Rev Cardiol* 7: 551–563, 2010.
21. **Munkhammar P, Carlsson M, Arheden H, Pesonen E.** Restrictive right ventricular physiology after tetralogy of Fallot repair is associated with fibrosis of the right ventricular outflow tract visualized on cardiac magnetic resonance imaging. *Eur Heart J Cardiovasc Imaging* 14: 978–985, 2013.
22. **Muzzarelli S, Ordovas KG, Cannavale G, Meadows AK, Higgins CB.** Tetralogy of Fallot: impact of the excursion of the interventricular septum on left ventricular systolic function and fibrosis after surgical repair. *Radiology* 259: 375–383, 2011.
23. **Ordovas KG, Carlsson M, Lease KE, Foster E, Meadows AK, Martin AJ, Hope M, Do L, Higgins CB, Saeed M.** Impaired regional left ventricular strain after repair of tetralogy of Fallot. *J Magn Reson Imaging* 35: 79–85, 2012.
24. **Pettersen E, Helle-Valle T, Edvardsen T, Lindberg H, Smith HJ, Smevik B, Smiseth OA, Andersen K.** Contraction pattern of the systemic right ventricle. *J Am Coll Cardiol* 49: 2450–2456, 2007.
25. **Riordan MM, Kovács SJ.** Elucidation of spatially distinct compensatory mechanisms in diastole: radial compensation for impaired longitudinal filling in left ventricular hypertrophy. *J Appl Physiol* 104: 513–520, 2008.
26. **Schwartz MC, Rome JJ, Gillespie MJ, Whitehead K, Harris MA, Fogel MA, Glatz AC.** Relation of left ventricular end diastolic pressure to right ventricular end diastolic volume after operative treatment of tetralogy of fallot. *Am J Cardiol* 109: 417–422, 2012.
27. **Sheehan F, Redington A.** The right ventricle: anatomy, physiology and clinical imaging. *Heart* 94: 1510–1515, 2008.
28. **Steding-Ehrenborg K, Carlsson M, Stephensen S, Arheden H.** Atrial aspiration from pulmonary and caval veins is caused by ventricular contraction and secures 70% of the total stroke volume independent of resting heart rate and heart size. *Clin Physiol Funct Imaging* 33: 233–240, 2013.
29. **Ugander M, Carlsson M, Arheden H.** Short-axis epicardial volume change is a measure of cardiac left ventricular short-axis function, which is independent of myocardial wall thickness. *Am J Physiol Heart Circ Physiol* 298: H530–H535, 2010.
30. **Wald RM, Redington AN, Pereira A, Provost YL, Paul NS, Oechslin EN, Silversides CK.** Refining the assessment of pulmonary regurgitation in adults after tetralogy of Fallot repair: should we be measuring regurgitant fraction or regurgitant volume? *Eur Heart J* 30: 356–361, 2008.
31. **Waters EA, Bowman AW, Kovács SJ.** MRI-determined left ventricular "crescent effect": a consequence of the slight deviation of contents of the pericardial sack from the constant-volume state. *Am J Physiol Heart Circ Physiol* 288: H848–H853, 2005.
32. **Zaffran S, Kelly RG, Meilhac SM, Buckingham ME, Brown NA.** Right ventricular myocardium derives from the anterior heart field. *Circ Res* 95: 261–268, 2004.